Creation and Destruction of Morphotropic Phase Boundaries through Electrical Poling: A Case Study of Lead-Free $(Bi_{1/2}Na_{1/2})TiO_3$-$BaTiO_3$ Piezoelectrics

Cheng Ma, Hanzheng Guo, Scott P. Beckman, and Xiaoli Tan*

Department of Materials Science and Engineering, Iowa State University, Ames, Iowa 50011, USA

(Received 15 March 2012; published 7 September 2012)

We report the first direct evidence that the morphotropic phase boundary in ferroelectric materials, along with the associated strong piezoelectricity, can be created, destroyed, or even replaced by another morphotropic phase boundary through phase transitions during electrical poling. The real-time evolution of crystal structure and domain morphology during the poling-induced phase transitions in $(Bi_{1/2}Na_{1/2})TiO_3$-$BaTiO_3$ is observed with *in situ* transmission electron microscopy. These observations elucidate the microstructural origin of the macroscopic piezoelectricity's dependence on the poling field and previously unexplained strain behaviors. This study demonstrates that the ferroelectric-to-ferroelectric transitions during the poling process can completely alter the morphotropic phase boundaries and, hence, must be comprehensively investigated when interpreting the microscopic mechanism of macroscopic piezoelectric behaviors.

DOI: 10.1103/PhysRevLett.109.107602 PACS numbers: 77.65.−j, 61.05.jm, 77.80.B−, 77.84.Cg

A material with coexisting energetically comparable states often displays extraordinary responses to external stimuli, such as large magnetostriction [1], giant electrocaloric effect [2], and colossal magnetoresistance [3]. In the case of piezoelectricity, ultrahigh piezoelectric responses are realized in compositions at the morphotropic phase boundary (MPB), where multiple ferroelectric phases with different crystal structures coexist [4–9]. Polycrystalline MPB materials must be poled by electric fields in order to exhibit piezoelectricity [4]. Under poling fields, the energy landscape of the constitutive polar phases in the MPB composition may be altered differently. Therefore, knowledge about the real-time evolution of crystal structures and domain morphologies during and after electrical poling is essentially important in understanding the physics of piezoelectricity.

However, in the past six decades, both theoretical and experimental studies have mainly focused on the virgin state of materials, prior to the application of a poling field [4–9]. Although different models on the piezoelectricity enhancement associated with MPBs have been proposed to describe interesting microscopic behaviors at zero field, the essential understanding of the microstructural mechanisms cannot be established without a complete picture of the *in situ* structural evolution under poling fields [10]. As a result, many fundamental questions have remained unanswered for decades: Will MPBs survive the strong poling fields? Can the poling field create an MPB in originally single-phase ferroelectrics? If poling fields can create or destroy MPBs, will such changes be preserved after the fields are removed? How does the change in MPBs during poling impact the macroscopic piezoelectric property?

Conclusive answers to these questions demand *in situ* real-time structural characterizations. There are two principal difficulties that hinder such studies. First, the crystal structures of different perovskite ferroelectric phases are frequently too similar to be well resolved by x-ray or neutron diffractions. It is particularly difficult to distinguish a material with coexisting phases from one single phase with a more complicated crystal structure. For example, there has been a continued debate on the microstructure of the MPB in $Pb(Zr, Ti)O_3$ (single monoclinic phase vs mixed rhombohedral and tetragonal phases) [5,6], the most important and widely studied piezoelectric compositions. Second, *in situ* application of electric fields in ferroelectric materials inevitably leads to a large piezoelectric strain and causes a complicated shifting of diffraction peaks [10]. Moreover, electric-field-induced domain texture must be taken into account in the structural analysis. These complications make the phase identification using x-ray or neutron diffractions particularly challenging.

These issues can be alleviated by using electric-field *in situ* transmission electron microscopy (TEM). Unlike x-ray or neutron diffraction, which obtains average structural information of materials, TEM is capable of precisely resolving the crystal structure of each individual phase among mixed phases through selected area electron diffraction. Furthermore, *in situ* TEM visualizes the real-time domain morphology changes under an electric field. However, electric-field *in situ* TEM requires very delicate sample preparation, and thus the number of such studies is still very limited [11–15].

In this Letter, direct evidence from *in situ* TEM experiments and corresponding piezoelectricity measurements provides conclusive answers to the questions raised above; we demonstrate that MPBs, and the enhanced piezoelectric response associated with them, can be either destroyed or created irreversibly during poling. Our first-principles calculations reveal that the ferroelectric phases are energetically close to each other, which corroborates the experimental conclusions.

One of the most extensively studied lead-free piezoelectrics, the $(1-x)(Bi_{1/2}Na_{1/2})TiO_3$-$xBaTiO_3$ solid solution [9,16–18], was selected to demonstrate the concept. In the virgin state, these ceramics crystallize in the rhombohedral $R3c$ ferroelectric phase for $x \leq 6\%$, the tetragonal $P4bm$ relaxor ferrielectric phase for $5\% \leq x \leq 11\%$, and the tetragonal $P4mm$ ferroelectric phase for $x \geq 10\%$ [19–21]. Therefore, a $R3c/P4bm$ MPB at $5\% \leq x \leq 6\%$ and a $P4bm/P4mm$ MPB at $10\% \leq x \leq 11\%$ exist in the unpoled state. Compared with results reported on poled ceramics [22–25], an irreversible $P4bm$-to-$P4mm$ phase transition is speculated to occur during poling for compositions with $x \geq 7\%$. We have recently confirmed this transition by *in situ* structural studies for $x = 7\%$ with poling fields up to 2.5 kV/mm [14]. However, the stability of the induced $P4mm$ phase in $x = 7\%$ against poling fields above 2.5 kV/mm is unknown. Any additional ferroelectric-to-ferroelectric transitions at higher fields may create an MPB in this composition. By the same token, electric-field-induced phase transitions in $5\% \leq x \leq 6\%$, if any, could possibly destroy the existing MPB. To verify these speculations, our study focuses on three compositions: $x = 5.5\%$, 6%, and 7%.

The preparation of $(Bi_{1/2}Na_{1/2})TiO_3$-$BaTiO_3$ ceramics and TEM specimens has been described elsewhere [20]. The electric-field *in situ* TEM technique is illustrated in Supplemental Material [26] and described in previous studies [12,13]. For each of the three compositions, over ten corroborating *in situ* TEM experiments were conducted. The piezoelectric coefficient d_{33} was measured on specimens poled at room temperature under fields from 1.5 to 6.5 kV/mm with increasing sequence of field levels.

The first-principles calculations were performed on the base compound $(Bi_{1/2}Na_{1/2})TiO_3$ by using the density functional theory methods encoded in the ABINIT software package [27]. The exchange-correlation energy was approximated by using the local density approximation [28]. In place of the all-electron ion potentials, projector augmented wave pseudopotentials were employed [29]. The plane wave expression of the wave function was truncated at 816 eV, and a Monkhorst-Pack [30] mesh was used to sample the Brillouin zone. For these calculations the forces on the atoms were converged to better than 10 meV/Å. The supercells used in the calculation were based on a superlattice constructed of alternating layers of $BiTiO_3$ and $NaTiO_3$ stacked in the [111] and [001] directions.

The *in situ* TEM results for $x = 6\%$ are displayed in Fig. 1. At zero field, consistent with previous studies [19,20], approximately 40% of the grains exhibit mixed $P4bm$ and $R3c$ phases (see Supplemental Material [26]), and the rest of the grains consist of $P4bm$ nanodomains only [Fig. 1(a)]. The $P4bm$ and $R3c$ symmetries are unambiguously determined from diffraction patterns: The $P4bm$ symmetry is characterized by the presence of $1/2\{ooe\}$ (o and e denote odd and even Miller indices, respectively) and the absence of $1/2\{ooo\}$ superlattice diffraction spots [Fig. 1(e)] and the $R3c$ symmetry by the presence of $1/2\{ooo\}$ and the absence of $1/2\{ooe\}$ spots [19–21,31–34]. A grain with

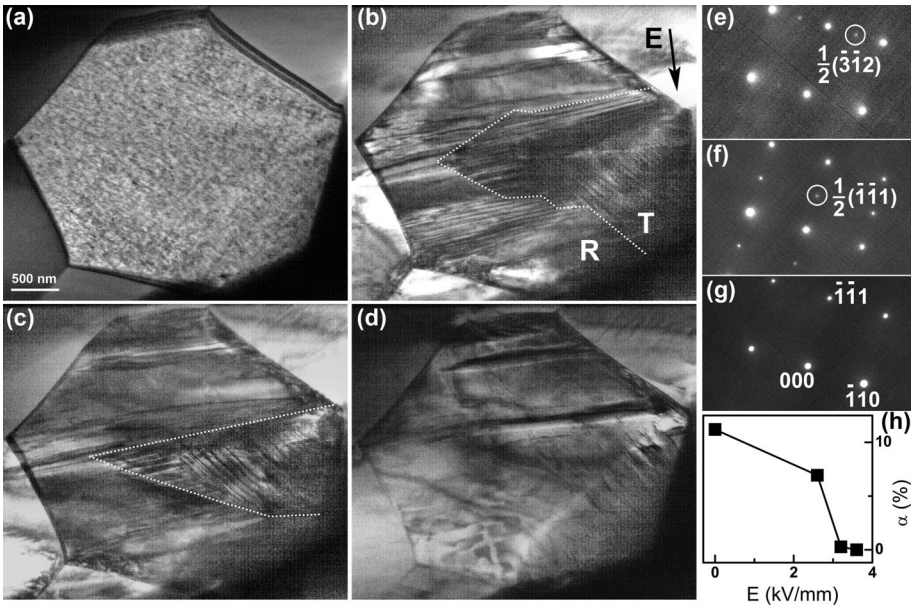

FIG. 1. TEM observations along the [112] zone axis of an originally phase-pure $P4bm$ grain in $x = 6\%$ under electric fields. (a) 0 kV/mm. (b) 3.2 kV/mm. The boundary between the volume with $R3c$ wedge-shaped domains (region R) and that with $P4mm$ lamellar domains (region T) is highlighted by bright dotted lines. The dark arrow indicates the direction of applied fields. (c) 3.6 kV/mm. (d) 4.0 kV/mm. Representative selected area electron diffraction patterns are displayed in (e) from nanodomains at 0 kV/mm, (f) from region R at 3.2 kV/mm, and (g) from region T at 3.6 kV/mm. The superlattice diffraction spots are indicated by bright circles. (h) The evolution of the intensity ratio $\alpha = I_{1/2(\bar{3}\,\bar{1}\,2)}/I_{(\bar{1}\,\bar{1}\,1)}$ with increasing applied fields.

pure $P4bm$ nanodomains [Fig. 1(a)] is examined in the *in situ* study. Under applied electric fields, these nanodomains coalesce into lamellar domains, and the $1/2\{ooe\}$ diffraction spots weaken. At 3.2 kV/mm a large part of the grain is taken by the wedge-shaped domains [region R in Fig. 1(b)], which are found to exhibit the $R3c$ symmetry [Fig. 1(f)]. At the same field level, the lamellar domains [region T in Fig. 1(b)] undergo a $P4bm$-to-$P4mm$ transition without any obvious change in the morphology, as demonstrated by the sudden decrease in the $1/2\{ooe\}$ spot intensity towards zero [Fig. 1(h)]. The region showing $R3c$ wedge-shaped domains expands with increasing field [Figs. 1(b) and 1(c)] and occupies the entire grain at 4.0 kV/mm [Fig. 1(d)]. Therefore, the application of electric fields creates an $R3c/P4mm$ MPB from the $P4bm$ phase for fields ranging between 3.2 and 3.6 kV/mm. Further increase in the field destroys the MPB through a $P4mm$-to-$R3c$ phase transition. These transitions during electrical poling are observed to be irreversible (see Supplemental Material [26]). As for the grains with mixed $P4bm$ and $R3c$ phases in the unpoled state, during poling the $P4bm$ phase shows the same phase transitions as those described above, while the originally existent $R3c$ phase does not experience any phase transitions. Consequently, the overall poling-induced phase transitions in the $x = 6\%$ ceramic can be described as $R3c/P4bm \rightarrow R3c/P4mm \rightarrow R3c$.

Prior to poling, the $x = 7\%$ ceramic is phase-pure with all the grains exhibiting $P4bm$ nanodomains [similar to those displayed in Fig. 1(a)]. The detailed *in situ* TEM results from 0 to 2.5 kV/mm were reported previously [14]; $P4bm$ nanodomains irreversibly transform to $P4mm$ lamellar domains under electric fields. With further increase in poling fields, the same electric-field-induced $P4mm$-to-$R3c$ transition as in $x=6\%$ is also seen in $x=7\%$ (see Supplemental Material [26]). Unlike $x=6\%$, this transition is not completed in $x = 7\%$ even under 4.0 kV/mm, the maximum field allowed by our *in situ* experimental device. The mixed $R3c$ and $P4mm$ phases remain after the applied fields are removed. The induced $R3c/P4mm$ MPB survives high poling fields.

The *in situ* TEM experiments were also performed on $x = 5.5\%$ (see Supplemental Material [26]). Almost all the grains of $x = 5.5\%$ exhibit mixed $R3c$ and $P4bm$ phases in the unpoled state. During poling the $P4bm$ phase irreversibly transforms into the $R3c$ phase; the poling process destroys the original $R3c/P4bm$ MPB.

The creation and destruction of MPBs during poling strongly correlates with the piezoelectric property measured from bulk ceramic samples, as shown in Fig. 2. The measured piezoelectric coefficient d_{33} for $x = 5.5\%$ is shown in Fig. 2(a) as a function of poling field E_{pol}. The increasing d_{33} is truncated by a plateau at a relatively low value of ~120 pC/N, because the $R3c/P4bm$ MPB transforms to a single $R3c$ phase before the field is high enough to fully pole the ceramic. The d_{33} for $x = 6\%$, shown in Fig. 2(b), reaches its maximum at a greater value of ~131 pC/N due to the replacement of the original $R3c/P4bm$ MPB by the $R3c/P4mm$ MPB at intermediate E_{pol}. However, at higher E_{pol} the d_{33} response diminishes, because the $R3c/P4mm$ MPB is destroyed. Figure 2(c) shows that d_{33} of $x = 7\%$ increases monotonically and reaches the maximum of 167 pC/N at the highest E_{pol} used in this study (6.5 kV/mm), which corresponds to the formation of a stable $R3c/P4mm$ MPB out of the single $P4bm$ phase during poling. Such excellent structure-property correlation is also evident across these

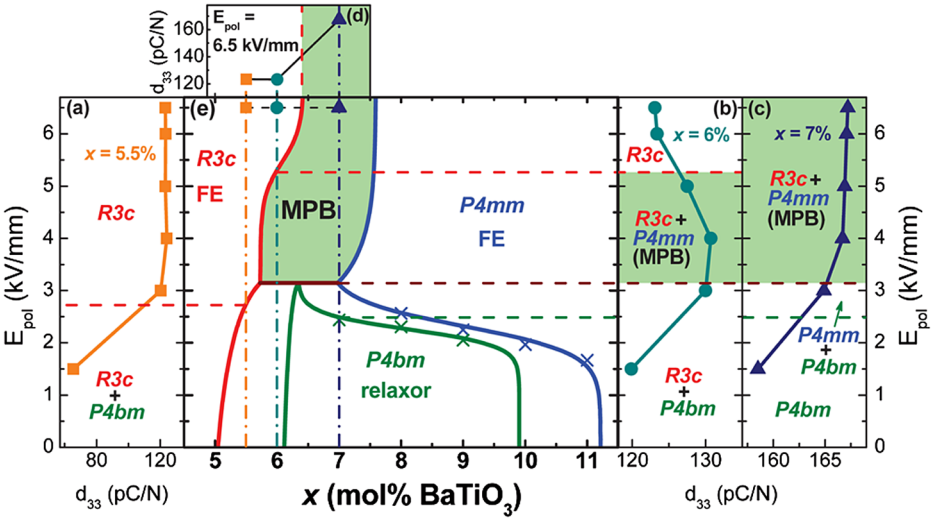

FIG. 2 (color online). The corresponding piezoelectric property d_{33} as a function of poling field E_{pol} is displayed for (a) $x = 5.5\%$, (b) $x = 6\%$, and (c) $x = 7\%$. (d) d_{33} as a function of composition at $E_{pol} = 6.5$ kV/mm. The error bars of the d_{33} data are smaller than the symbols and hence not shown. (e) The proposed E_{pol} vs x phase diagram for $(1-x)(Bi_{1/2}Na_{1/2})TiO_3$-$xBaTiO_3$. FE stands for ferroelectric. The electric-field-induced $R3c/P4mm$ MPB giving rise to enhanced piezoelectricity is emphasized with green shading.

three compositions at the same E_{pol}, as shown in Fig. 2(d). The compositions with $x = 5.5\%$ and 6%, both exhibiting the single $R3c$ phase after poling at 6.5 kV/mm, possess almost identical d_{33} values, whereas the composition $x = 7\%$, exhibiting the $R3c/P4mm$ MPB after poling, shows a much higher d_{33}.

An E_{pol} vs x phase diagram for the $(1-x)(Bi_{1/2}Na_{1/2})TiO_3$-$xBaTiO_3$ binary system can be constructed to summarize the evolution of phases with poling fields at room temperature [Fig. 2(e)]. The critical fields in this diagram are estimated with bulk samples from the d_{33} results in this study [Figs. 2(a)–2(c)] and from the volume strain measurements in a previous study [35]. The $R3c/P4bm$ and the $P4bm/P4mm$ MPBs converge as E_{pol} is increased. The horizontal "isofield" line, where $R3c$, $P4bm$, and $P4mm$ phases coexist, truncates the convergence. Further increase in E_{pol} results in an $R3c/P4mm$ MPB. This phase diagram points out that the MPB can be destroyed ($x = 5.5\%$ and 6%), created ($x = 7\%$), or even replaced by another MPB ($x = 6\%$) during poling. It unambiguously demonstrates the importance of poling-induced phase transitions in interpreting the microscopic origin of macroscopic piezoelectric behaviors.

The transition from the $P4bm$ phase to the $R3c$ or $P4mm$ ferroelectric phase is believed to be directly driven by the poling field. Its physical mechanism is presumably similar to that of an electric-field-induced antiferroelectric-to-ferroelectric transition, since the ferrielectric $P4bm$ structure exhibits antiparallel cation displacements in its unit cell [14,33]. However, the $P4mm$-to-$R3c$ ferroelectric-to-ferroelectric transition, as observed in $x = 6\%$ and 7% at higher poling fields, may not be directly driven by electric fields, because it depends very little on the direction of the applied field with respect to a specific grain during the *in situ* TEM experiment. As in other solid solution systems [36], the piezoelectric strain developed under the applied field may have played a critical role in facilitating the phase transition.

Despite the different driving forces, these complex phase transitions are expected to trace their origin in the base compound $(Bi_{1/2}Na_{1/2})TiO_3$. The results from our rudimentary first-principles calculations are summarized in the energy vs volume plots shown in Fig. 3, and details are given in Supplemental Material [26]. The ground state of $(Bi_{1/2}Na_{1/2})TiO_3$ is the $R3c$ ferroelectric phase, consistent with the experimental observation [33], while the $P4mm$ and $P4bm$ phases have energies very close to the $R3c$ phase. It is found that for the [111] superlattice structure the $P4mm$ and $P4bm$ phases are equienergetic but differ in volume. Presumably, the oxygen octahedra tilting facilitates the $P4bm$ phase having a more compact structure. These calculations suggest that it is possible to stabilize different polar phases by controlling the composition, strain, or applied electric field. The calculations also correctly predict the trend in the unit cell volume of different polar phases in

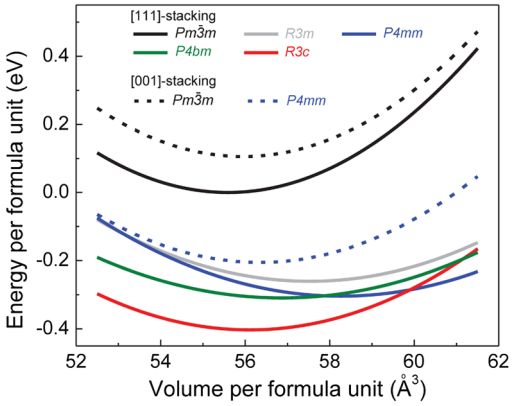

FIG. 3 (color online). First-principles calculations of the energies of different perovskite variants for the base compound $(Bi_{1/2}Na_{1/2})TiO_3$. The energy of the cubic phase with a [111] stacking superlattice is arbitrarily defined as the energy zero.

$(Bi_{1/2}Na_{1/2})TiO_3$ [33]. Assuming this trend is preserved in the $(1-x)(Bi_{1/2}Na_{1/2})TiO_3$-$xBaTiO_3$ binary system on the $(Bi_{1/2}Na_{1/2})TiO_3$-rich side (e.g. $x < 10\%$), the electric-field-induced phase transition sequence ($R3c/P4bm \rightarrow R3c/P4mm \rightarrow R3c$) revealed by our *in situ* TEM experiment on $x = 6\%$ explains very well the cusp-shaped anomaly in the volume strain vs E_{pol} curve at the intermediate field level in this composition [35]. Finally, it should be noted that the presence of multiple energetically comparable ferroelectric phases is not unique for $(Bi_{1/2}Na_{1/2})TiO_3$; it is common for many perovskite compounds due to the flexibility of the perovskite structure [4–9]. The creation and destruction of MPBs during electrical poling may likely occur in other perovskite ferroelectric systems. Our results will profoundly change the research of piezoelectric materials. Specifically, single-phase compositions, which were largely excluded before, may also exhibit superior piezoelectricity if stable MPBs form during poling.

In conclusion, our *in situ* TEM experiments, supported by piezoelectric property measurements from bulk samples, have unambiguously demonstrated that poling fields may irreversibly destroy or create MPBs and the associated piezoelectricity enhancement. The results point out that, in addition to the virgin-state phase structure, the ferroelectric-to-ferroelectric phase transitions during poling must also be comprehensively studied to fully understand the microstructural mechanism of the macroscopic piezoelectric behaviors. The discovery reported here could inspire new directions in the research in other fields where competing energetically comparable states are critical, such as magnetostrictive [1] and electrocaloric effects [2].

The National Science Foundation (NSF), through Grant No. DMR-1037898, supported this work. TEM experiments were performed at the Ames Laboratory, which is operated for the U.S. Department of Energy by Iowa State University under Contract No. DE-AC02-07CH11358.

*Corresponding author.
xtan@iastate.edu

[1] S. Yang, H. Bao, C. Zhou, Y. Wang, X. Ren, Y. Matsushita, Y. Katsuya, M. Tanaka, K. Kobayashi, X. Song, and J. Gao, Phys. Rev. Lett. **104**, 197201 (2010).
[2] A. S. Mischenko, Q. Zhang, J. F. Scott, R. W. Whatmore, and N. D. Mathur, Science **311**, 1270 (2006).
[3] E. Dagotto, *Nanoscale Phase Separation and Colossal Magnetoresistance* (Springer-Verlag, New York, 2003).
[4] B. Jaffe, W. R. Cook, and H. Jaffe, *Piezoelectric Ceramics* (Academic, London, 1971).
[5] R. Guo, L. E. Cross, S.-E. Park, B. Noheda, D. E. Cox, and G. Shirane, Phys. Rev. Lett. **84**, 5423 (2000).
[6] K. A. Schonau, L. A. Schmitt, M. Knapp, H. Fuess, R.-A. Eichel, H. Kungl, and M. J. Hoffmann, Phys. Rev. B **75**, 184117 (2007).
[7] D. Phelan, X. Long, Y. Xie, Z.-G. Ye, A. M. Glazer, H. Yokota, P. A. Thomas, and P. M. Gehring, Phys. Rev. Lett. **105**, 207601 (2010).
[8] W. Liu and X. Ren, Phys. Rev. Lett. **103**, 257602 (2009).
[9] J. Rödel, W. Jo, K. T. P. Seifert, E. M. Anton, T. Granzow, and D. Damjanovic, J. Am. Ceram. Soc. **92**, 1153 (2009).
[10] M. Hinterstein, J. Rouquette, J. Haines, Ph. Papet, M. Knapp, J. Glaum, and H. Fuess, Phys. Rev. Lett. **107**, 077602 (2011).
[11] Y. Sato, T. Hirayama, and Y. Ikuhara, Phys. Rev. Lett. **107**, 187601 (2011).
[12] X. Tan, Z. Xu, J. K. Shang, and P. Han, Appl. Phys. Lett. **77**, 1529 (2000).
[13] H. He and X. Tan, Phys. Rev. B **72**, 024102 (2005).
[14] X. Tan, C. Ma, J. Frederick, S. Beckman, and K. G. Webber, J. Am. Ceram. Soc. **94**, 4091 (2011).
[15] C. A. Randall, D. J. Barber, and R. W. Whatmore, J. Microsc. **145**, 275 (1987).
[16] J. Yao, L. Yan, W. Ge, L. Luo, J. Li, D. Viehland, Q. Zhang, and H. Luo, Phys. Rev. B **83**, 054107 (2011).
[17] F. Cordero, F. Craciun, F. Trequattrini, E. Mercadelli, and C. Galassi, Phys. Rev. B **81**, 144124 (2010).
[18] W. Jo, J. E. Daniels, J. L. Jones, X. Tan, P. A. Thomas, D. Damjanovic, and J. Rödel, J. Appl. Phys. **109**, 014110 (2011).
[19] C. Ma and X. Tan, Solid State Commun. **150**, 1497 (2010).
[20] C. Ma, X. Tan, E. Dul'kin, and M. Roth, J. Appl. Phys. **108**, 104105 (2010).
[21] C. Ma and X. Tan, J. Am. Ceram. Soc. **94**, 4040 (2011).
[22] T. Takenaka, K. Maruyama, and K. Sakata, Jpn. J. Appl. Phys. **30**, 2236 (1991).
[23] Y. Hiruma, H. Nagata, and T. Takenaka, J. Appl. Phys. **104**, 124106 (2008).
[24] J. E. Daniels, W. Jo, J. Rödel, and J. L. Jones, Appl. Phys. Lett. **95**, 032904 (2009).
[25] H. Simons, J. Daniels, W. Jo, R. Dittmer, A. Studer, M. Avdeev, J. Rödel, and M. Hoffman, Appl. Phys. Lett. **98**, 082901 (2011).
[26] See Supplemental Material at http://link.aps.org/supplemental/10.1103/PhysRevLett.109.107602 for the configuration of the *in situ* TEM experiment, the grain with mixed $R3c$ and $P4mm$ phases in $x = 6\%$, the irreversibility of electric-field-induced phase transitions, the electric-field *in situ* TEM results of $x = 7\%$ and 5.5%, and detailed results of the *ab initio* calculations.
[27] W. Kohn and L. J. Sham, Phys. Rev. **140**, A1133 (1965).
[28] D. M. Ceperley and B. J. Alder, Phys. Rev. Lett. **45**, 566 (1980).
[29] P. E. Blochl, Phys. Rev. B **50**, 17 953 (1994).
[30] H. J. Monkhorst and J. D. Pack, Phys. Rev. B **13**, 5188 (1976).
[31] A. M. Glazer, Acta Crystallogr. Sect. A **31**, 756 (1975).
[32] D. I. Woodward and I. M. Reaney, Acta Crystallogr. Sect. B **61**, 387 (2005).
[33] G. O. Jones and P. A. Thomas, Acta Crystallogr. Sect. B **58**, 168 (2002).
[34] V. Dorcet and G. Trolliard, Acta Mater. **56**, 1753 (2008).
[35] W. Jo and J. Rödel, Appl. Phys. Lett. **99**, 042901 (2011).
[36] X. Tan, J. Frederick, C. Ma, W. Jo, and J. Rödel, Phys. Rev. Lett. **105**, 255702 (2010).